

# Theory and simulation of strong correlations in quantum Coulomb systems

M Bonitz<sup>1</sup>, D Semkat<sup>1</sup>, A Filinov<sup>1</sup>, V Golubnychyi<sup>1</sup>, D Kremp<sup>1</sup>,  
D O Gericke<sup>2</sup>, M S Murillo<sup>2</sup>, V Filinov<sup>3</sup>, V Fortov<sup>3</sup>, W Hoyer<sup>4</sup>  
and S W Koch<sup>4</sup>

<sup>1</sup> Fachbereich Physik, Universität Rostock, D-18051 Rostock, Germany

<sup>2</sup> Theoretical Division, Los Alamos National Laboratory, Los Alamos, NM 87545, USA

<sup>3</sup> Institute for High Energy Density, Russian Academy of Sciences, Izhoroskay 13/19,  
Moscow 127412, Russia

<sup>4</sup> Fachbereich Physik und Zentrum für Materialwissenschaften, Philipps-Universität Marburg,  
D-35032 Marburg, Germany

E-mail: michael.bonitz@physik.uni-rostock.de

Received 22 October 2002

Published 22 May 2003

Online at [stacks.iop.org/JPhysA/36/5921](http://stacks.iop.org/JPhysA/36/5921)

## Abstract

Strong correlations in quantum Coulomb systems (QCS) are attracting increasing interest in many fields ranging from dense plasmas and semiconductors to metal clusters and ultracold trapped ions. Examples are bound states in dense plasmas (atoms, molecules, clusters) and semiconductors (excitons, trions, biexcitons) or Coulomb crystals. We present first-principle simulation results of these systems including path integral Monte Carlo simulations of the equilibrium behaviour of dense hydrogen and electron–hole plasmas and molecular dynamics and quantum kinetic theory simulations of the nonequilibrium properties of QCS. Finally, we critically assess potential and limitations of the various methods in their application to Coulomb systems.

PACS numbers: 05.30.–d, 52.65.–y

(Some figures in this article are in colour only in the electronic version)

## 1. Introduction

The family of Coulomb systems, i.e. many-body systems which are dominated by Coulomb interaction, has grown beyond conventional plasmas in space or laboratory for many years, for an overview, see e.g. [1–3]. They also include electron–hole plasmas in semiconductors, the electron gas in metals, charged particles confined in various traps or storage rings, charged complex or dust particles and also small few-particle clusters in mesoscopic quantum dots. Despite their different nature, all Coulomb systems have similar fundamental properties which

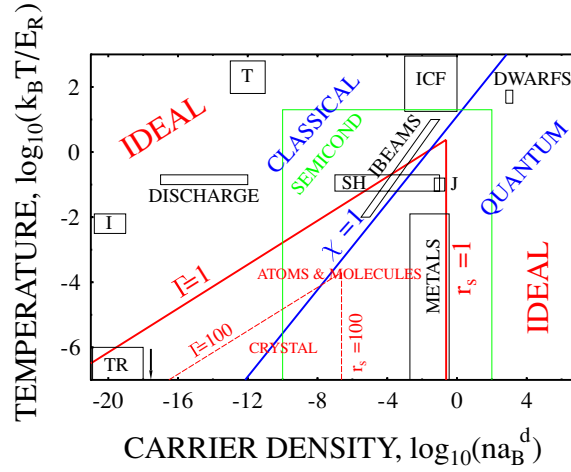


**Figure 1.** Universal density–temperature plane for Coulomb systems in equilibrium. The lines  $\Gamma = 1$  and  $r_s = 1$  enclose the region of strong Coulomb correlations, the lines  $\Gamma = 100$  and  $r_s = 100$  give an approximate boundary for Coulomb (Wigner) crystals. The line  $\chi = 1$  separates classical (left) and quantum (right) systems. Abbreviations stand for CS in tokamaks (T), inertial confinement fusion (ICF), brown dwarf stars (DWARFS), Jupiter interior (J), ionosphere (I), shock wave plasmas (SH), ion beams (IBEAMS). The green box denotes the region of semiconductors (scaled with the excitonic  $a_B, E_R$ ). Plasmas in traps (TR) are outside the figure, typically at sub-Kelvin temperatures.

are governed by two parameters: the strength of the Coulomb interaction (measured by the coupling parameters  $\Gamma$  and  $r_s$ ) and the strength of quantum effects (degeneracy parameter  $\chi$ ). These parameters are determined by the ratio of characteristic energy and length scales [4, 5]:

- *Length scales:* (1)  $\bar{r}$  is the average interparticle distance,  $\bar{r} \sim n^{-d}$  ( $n$  and  $d$  denote the density and dimensionality,  $d = 1, 2, 3$  of the system respectively). (2)  $\Lambda$  is the quantum-mechanical extension of the particles. For free particles,  $\Lambda = h/\sqrt{2\pi mk_B T}$  (DeBroglie wavelength), for bound particles  $\Lambda$  is given by the extension of the wavefunction. (3) The relevant Bohr radius  $a_B = \frac{\epsilon}{e_a e_b} \frac{\hbar^2}{m_{ab}}$ , with  $m_{ab}^{-1} = m_a^{-1} + m_b^{-1}$ .
- *Energy scales:* (1)  $\langle K \rangle$  is the mean kinetic energy, in a classical system  $\langle K \rangle_{cl} = \frac{d}{2} k_B T$ , whereas in a highly degenerate Fermi system  $\langle K \rangle_{qm} = \frac{3}{5} E_F$  ( $E_F$  denotes the Fermi energy); (2) the mean Coulomb energy—for free particles:  $\langle U_c \rangle_f = \frac{e_a e_b}{4\pi\epsilon} \frac{1}{\bar{r}}$ , and for bound particles:  $\langle U_c \rangle_B = \frac{e_a e_b}{4\pi\epsilon} \frac{1}{2a_B} \equiv E_R$  (Rydberg).
- The *degeneracy parameter*  $\chi \equiv n\Lambda^d \sim (\Lambda/\bar{r})^d$  divides many-body systems into classical ( $\chi < 1$ ) and quantum-mechanical ones ( $\chi \geq 1$ ).
- The *Coulomb coupling parameter* is the ratio  $|\langle U_c \rangle|/\langle K \rangle$ . For classical systems  $\Gamma \equiv |\langle U_c \rangle|/k_B T$ , whereas for quantum systems the role of  $\Gamma$  is taken over by  $r_s \equiv \bar{r}/a_B \sim |\langle U_c \rangle|/E_F$ .

Figure 1 shows a qualitative phase diagram of Coulomb systems in equilibrium as a function of temperature and density. It allows us to compare different Coulomb systems and projects results from one area onto another. One simply has to rescale length and energies in the actual  $a_B$  and  $E_R$  using the corresponding data for  $m, e, d$  and  $\epsilon$ . As an illustrative example, figure 1 shows that the electron–hole plasma in semiconductors covers a remarkably broad range of situations in laboratory and space plasmas.

## 2. Coulomb structures in equilibrium

The general behaviour is well known: in the limit of high temperature,  $\chi \ll 1$  and  $\Gamma \ll 1$ , CS behave as a classical ideal gas of free charge carriers. Similarly, in the limit of high densities,  $\chi \gg 1$  and  $r_s \ll 1$ , ideal gas behaviour is recovered, however, that of a quantum gas of spatially extended mutually penetrating particles. Both limits are structureless and comparatively simple theoretically: they are successfully (and rigorously) treated by perturbation theory (with respect to  $\Gamma$  or  $r_s$ ). Much more interesting behaviour emerges when the Coulomb energy starts to exceed the kinetic energy, i.e.  $\Gamma \geq 1$  or  $r_s \geq 1$ —the behaviour of charged particles is then strongly correlated, electrons may become trapped by ions leading to the formation of atoms, molecules and macroscopic matter. This parameter range is very challenging theoretically due to the absence of small expansion parameters. Traditional classical and quantum-statistical methods, e.g. [4–7], are able to describe only certain types of these correlations by summing special classes of diagrams (such as ladder-type diagrams describing atoms or excitons).

The alternative here is first-principle simulations such as path integral Monte Carlo (PIMC) which do not have restrictions with respect to the coupling strengths, e.g. [8–10]. Figure 2 shows direct fermionic PIMC simulations for an excited electron–hole plasma in a semiconductor quantum well in the range of strong correlations. Both electrons and holes are strongly degenerate, i.e.  $\chi_{e,h} > 1$ , thus a quantum-mechanical treatment is essential. The PIMC simulations yield the correct size of the electrons and holes (the dots indicate the average extension of the wavefunction). If the density is increased (from top left to the bottom right figure), this size becomes comparable to, and even exceeds, the mean interparticle distance as shown by the overlapping dots. The temperature is chosen well below the exciton binding energy, and the formation of localized electron–hole pairs (excitons), three-particle complexes (trions), molecules (bi-excitons) is evident at low density (large  $r_s$ ). With increasing density (bottom figures), even larger complexes form—electron–hole droplets which have been predicted by Keldysh more than three decades ago and observed experimentally, see [11] for more details on these effects and the simulations.

Very similar situations exist in dense plasmas found in the interior of the giant planets, brown dwarf stars or in plasma compression experiments (cf figure 1). Similarly, also the PIMC simulations can be directly applied to these systems, and results for dense hydrogen are shown in figure 3. Obviously, the main difference is the much larger mass ratio of ions and electrons compared to electron–hole systems, which allows us to treat the ions classically (i.e. as point-like particles, they are shown by blue dots in the figure). In contrast, the electrons are treated quantum-mechanically fully including diffraction effects (finite extension, given by the size of the clouds of small dots) and fermionic exchange (red and green colours denote electrons with different spin projections). The peculiar feature shown in the top figures is the formation of large clusters which contain several protons embedded into de-localized electrons. This is very similar to the electron–hole droplets (cf figure 2) and indicates an instability of the homogeneous plasma state at low temperature which may be related to the hypothetical plasma phase transition, e.g. [11–13]. As the density is increased further (bottom figures) the electron extension  $\Lambda$  exceeds the Bohr radius and bound states and clusters become unstable. The bottom left figures show a high-density liquid-like plasma state. Further increase of the density by two orders of magnitude leads to an unusual state where the electrons behave as a completely delocalized weakly interacting quantum gas ( $\chi_e \gg 1$ ,  $r_s \ll 1$ ); the protons, however, are still classical ( $\chi_p < 1$ ) but so strongly coupled ( $\Gamma > 175$ ) that they form a Wigner lattice embedded into the electron gas (see the bottom right figure). Such behaviour is expected to occur in high-density stellar objects, and it is very encouraging that PIMC simulations are able to correctly reproduce it. Still these simulations of fermions at high

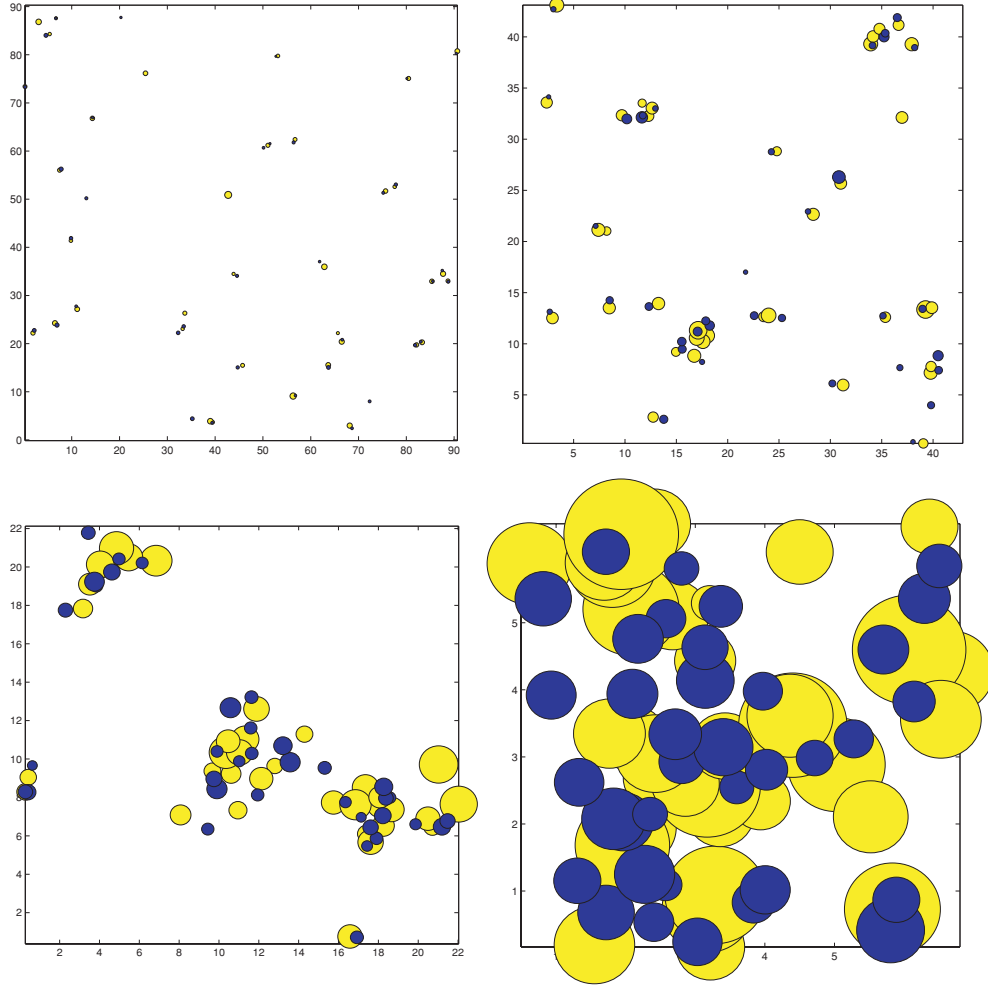


**Figure 2.** Snapshots of a correlated quantum electron-hole plasma in a two-dimensional semiconductor quantum well at low temperature  $T = 0.1 E_R$  simulated with path integral Monte Carlo. The densities are:  $r_s = 8.6$  (top left),  $r_s = 4.2$  (top right),  $r_s = 2.1$  (bottom left) and  $r_s = 0.6$  (bottom right). Yellow (blue) dots show the average quantum extension of an electron (hole).

density are in their infancy which is due to the fermion sign problem, e.g. [9]. A solution of this problem for strongly correlated Coulomb systems, either by appropriate additional approximations (restricted PIMC, e.g. [14]) or direct simulations [9, 11, 15, 16] remains a major challenge in the theory of quantum Coulomb systems.

### 3. Nonequilibrium theory of correlated Coulomb systems

A theoretical description of Coulomb systems starts from the Hamiltonian

$$\hat{H} = \hat{K} + \hat{U}_c + \hat{U}_{\text{ext}} \quad \hat{K} = - \sum_{i=1}^N \frac{\hbar^2 \nabla_i^2}{2m_i} \quad \hat{U}_c = \sum_{i<j}^N \frac{e_i e_j}{\epsilon |\vec{r}_i - \vec{r}_j|} \quad (1)$$

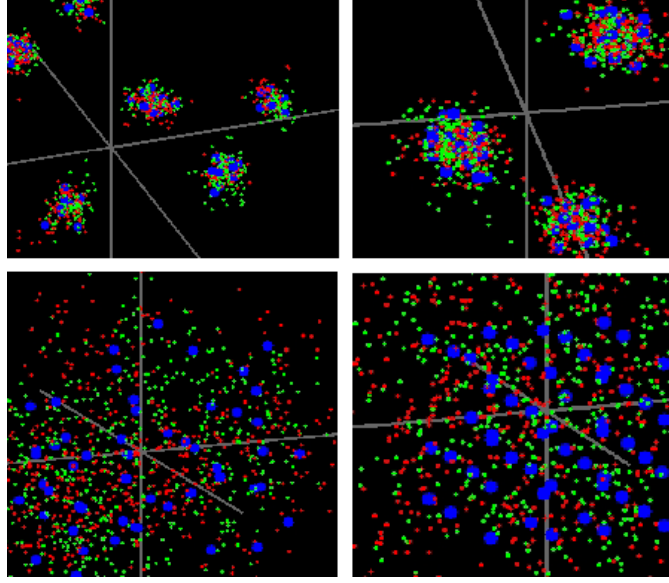


**Figure 3.** PIMC simulation snapshots of strongly correlated hydrogen plasma at  $T = 10\,000$  K in 3D space (grey lines are the coordinate axes). Electrons are shown by clouds of small dots, red and green dots denote electrons with different spin projections. The protons are treated classically and marked by large blue dots. Densities are:  $n = 10^{22} \text{ cm}^{-3}$  (top left figure),  $n = 3 \times 10^{22} \text{ cm}^{-3}$  (top right),  $10^{24} \text{ cm}^{-3}$  (bottom left) and  $10^{26} \text{ cm}^{-3}$  (bottom right). Scales on the axes are increased with density according to  $\bar{r} \sim n^{(-1/3)}$ .

where  $K$ ,  $U_c$  and  $U_{\text{ext}}$  denote the kinetic energy, Coulomb interaction energy and energy due to external fields. Equilibrium theories are derived from the  $N$ -particle density operator  $\hat{\rho}_N = e^{-\hat{H}/kT}$  which, for Fermi systems, has to be properly anti-symmetrized. Any observable can be computed from the density operator, e.g. [4, 5] by using quantum-statistical or simulation methods. In particular, PIMC methods are able to yield first-principle results of the equilibrium properties of CS. However, so far no comparably powerful method exists for time-dependent (dynamical, transport, optical) properties which require solution of the equation of motion of the density operator, the von Neumann equation,

$$i\hbar \frac{\partial}{\partial t} \hat{\rho}_N(t) - [\hat{H}, \hat{\rho}_N(t)] = 0. \quad (2)$$

An exception is classical Coulomb systems where equation (2) reduces to the equations of classical mechanics (Newton's equations) which can be integrated directly (molecular dynamics, MD). There exist various attempts to extend MD to *quantum* Coulomb systems three of which will be mentioned here. The first is the concept of wave packet MD [17, 18] where one computes quasi-classical phase-space trajectories of particles which are represented by a wave packet of finite extension in coordinate and momentum space. A second approach is quasi-classical MD (QCMD) where one retains (in the dynamics) the point size of the particles but includes quantum effects into a modified interaction potential which takes into account quantum extension effects at small inter-particle distances (see section 3.1 and [19]). As a third approach we mention the Wigner function MD (WFMD) where equation (2) is transformed to the Wigner representation and solved directly for the  $N$ -particle density matrix  $\rho(R_1, p_1, \dots, R_N, p_N)$  (see e.g. [21, 22]).

Besides these particle-based methods there exist powerful quantum kinetic approaches [4–6]. There, the equation for  $\rho_N$  is transformed into a kinetic equation for the single-particle density operator  $\rho_1 \equiv \text{Tr}_{2\dots N} \rho_N$ , the one-particle Wigner function  $f(R, p, t)$ , or the one-particle Green functions  $G^{\lessgtr}$ . The latter are defined by

$$G^<(\mathbf{k} + \mathbf{q}, t_1; \mathbf{k}, t_2) = i\langle a_{\mathbf{k}}^\dagger(t_2) a_{\mathbf{k}+\mathbf{q}}(t_1) \rangle \quad G^>(\mathbf{k} + \mathbf{q}, t_1; \mathbf{k}, t_2) = -i\langle a_{\mathbf{k}+\mathbf{q}}(t_1) a_{\mathbf{k}}^\dagger(t_2) \rangle \quad (3)$$

where the field operators  $a_{\mathbf{k}+\mathbf{q}}(t_1)$  and  $a_{\mathbf{k}}^\dagger(t_2)$  denote annihilation of a particle with momentum  $\mathbf{k} + \mathbf{q}$  at time  $t_1$  and creation of a particle with momentum  $\mathbf{k}$  at time  $t_2$ , respectively, which assure exact fulfillment of the Fermi statistics. The equations of motion for  $G^{\lessgtr}$  are the Kadanoff–Baym/Keldysh equations (KBE) [4, 7, 23–25],

$$\begin{aligned} \left( i\hbar \frac{\partial}{\partial t_1} - \epsilon_{\mathbf{k}} \right) G^{\lessgtr}(\mathbf{k}_1 t_1; \mathbf{k}_2 t_2) - \sum_{\mathbf{q}} U_{\text{ext}}(-\mathbf{q}, t_1) G^{\lessgtr}(\mathbf{k}_1 - \mathbf{q}, t_1; \mathbf{k}_2 t_2) \\ = \sum_{\bar{\mathbf{k}}} \Sigma^{\text{HF}}(\mathbf{k}_1 t_1; \bar{\mathbf{k}} t_1) G^{\lessgtr}(\bar{\mathbf{k}} t_1; \mathbf{k}_2 t_2) + I^{\lessgtr}(\mathbf{k}_1 t_1; \mathbf{k}_2 t_2) \end{aligned} \quad (4)$$

(to be supplemented with the adjoint equation), where  $\Sigma^{\text{HF}}$  is the Hartree–Fock self-energy, and the collision integrals  $I^{\lessgtr}$  contain the short-range correlation effects (see below).

The advantage of these methods is that quantum and spin effects are built in rigorously. The problem, on the other hand, is the difficult (or inefficient) treatment of strong correlations, as in the equilibrium case. Here, it manifests itself in the familiar fact that the equations for  $f$  or  $G^{\lessgtr}$  are not closed but couple to the equations of motion for the two-particle function  $f_{12}$  or  $G_{12}$  and so on, giving rise to a hierarchy of equations (BBGKY-hierarchy of reduced density operators, e.g. [5] or Martin–Schwinger hierarchy of the Green functions [4–6]). Solution of the kinetic equation requires decoupling of the hierarchy which is related to an approximate treatment of correlation effect. To solve equation (4), a formal closure is performed by introducing a self-energy according to  $\text{Tr}_2 V_{12} G_{12} = \Sigma_1 G_1$ . Below we show results where  $\Sigma_1$  is used in the static Born approximation.

Finally, we point out that the KBE have several important advantages compared to conventional kinetic equations (CKE, such as the Boltzmann, Landau or Vlasov equation): they *conserve total energy* (kinetic and correlation energy) whereas CKE conserve only kinetic energy and they describe relaxation to a *correlated equilibrium* state whereas CKE always yield an ideal equilibrium (given by a Maxwell or Fermi/Bose distribution function). These properties are crucial in the description of relaxation processes in correlated Coulomb systems, such as laser plasmas [26, 27] or optically excited semiconductors [28–30]. Besides the KBE, these requirements are also fulfilled by classical MD simulations (with the noted above problems in handling quantum and spin effects).

### 3.1. Dynamical properties. Plasmon spectrum

As a first example of nonequilibrium properties of quantum Coulomb systems we consider dielectric properties. Oscillations of weakly correlated plasmas have been investigated in extraordinary detail during the last half century, the standard result for uncorrelated classical and quantum plasmas is given by the Vlasov approximation and random phase approximation (RPA), respectively. Similarly as for the equilibrium properties (section 2), CS show also universal dynamical behaviour: the long-range Coulomb interaction gives rise to a characteristic timescale, the plasma period  $T_{\text{pl}} = 2\pi/\omega_{\text{pl}}$ , where  $\omega_{\text{pl}}^2 = 4\pi n e^2 / (\epsilon m)$ .  $\omega_{\text{pl}}$  is the universal eigenfrequency of a macroscopic three-dimensional classical or quantum one-component plasma and is not affected by short-range correlations. On the other hand, correlation and quantum effects influence the frequency of plasma oscillations of finite range

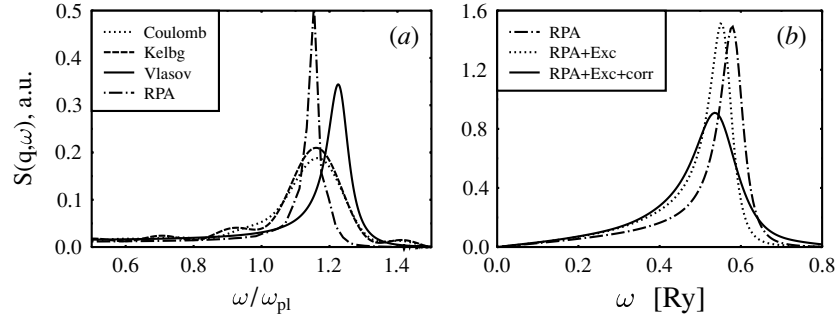


**Figure 4.** Dynamic structure factor of a correlated quantum electron gas for a fixed wave number. The figure compares standard models which neglect correlations (RPA and Vlasov) with two first-principle simulations which conserve density and total energy: classical molecular dynamics (a) and quantum kinetic theory (b).

(finite wavenumber  $q$ ), leading to a reduction of the frequency and to an increased damping. To compute these effects requires to go beyond the Vlasov and RPA level which has been proven difficult since a number of consistency requirements—most importantly sum rules—have to be fulfilled.

One approach that meets these requirements is quantum kinetic equations. It has been demonstrated that due to conservation of total energy (and density) the solution of the KBE (4) with a monochromatic external excitation  $U_{\text{ext}} = U(t) \cos q_0 t$  includes the required set of correlation corrections (self-energy and vertex terms) self-consistently and guarantees sum rule preservation [4, 23]. Figure 4(b) shows, for a fixed wave number  $q_0$ , the result of correlations and fermionic exchange (full line) in comparison to the RPA [23]. The second approach capable of yielding rigorous results for the plasmon spectrum of correlated CS is molecular dynamics (e.g. [19, 20]). Figure 4(a) shows results of classical MD with a quantum potential [19], the Kelbg potential,

$$U_{\text{KELBG}}(r, T) = 4\pi e^2 \left( \frac{1 - \exp(-r^2/\lambda^2)}{r} + \frac{\sqrt{\pi}}{\lambda} \text{erfc}(r/\lambda) \right) \quad (5)$$

where  $\lambda(T) = \Lambda/\sqrt{2\pi}$ .  $U_{\text{KELBG}}$  correctly takes into account quantum diffraction effects (in particular it has a finite height at zero  $r$ ) and, at large distances, approaches the Coulomb potential. Figure 4(a) shows that correlations lead to an additional damping of the plasmon (increased width of the peak) and a reduction of its energy, thereby also preserving sum rules [19]. Further development of this QCMD approach and its extension to strong coupling and strong degeneracy are possible by the derivation of improved quantum potentials [31].

### 3.2. Short-time dynamics. Plasma cooling

Let us now consider rapid processes in correlated CS which proceed on the timescale of the plasma period  $T_{\text{pl}}$ . This is the time necessary to correlate the particles after the plasma is being created—the time to build up the pair distribution function, the plasmon spectrum and the screening cloud [4, 28, 32, 33]. This build up of correlations among initially independent (uncorrelated) particles is shown in figure 5: the magnitude of Coulomb interaction (and kinetic) energy increases during a short initial period and remains constant for  $t \gtrsim T_{\text{pl}}$ .

Now it is interesting to ask if one can achieve the opposite: bring the plasma into a state which is *overcorrelated* [5, 34]. As a consequence, the magnitude of correlation energy would



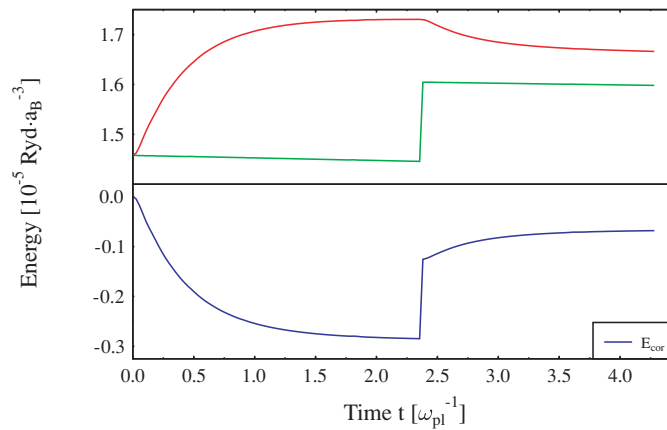


**Figure 5.** Energy relaxation in a one-component plasma before and after a sudden reduction of the interaction from solution of the KBE (4). Initially, correlations are being built up, causing heating of the system. After reduction of the interaction correlations are being reduced, the plasma cools [29]. Blue (red)—correlation (kinetic) energy, green—total (kinetic and correlation) energy.

**Table 1.** Critical assessment of strengths (increasing from ‘–’ to ‘+++’) and limitations of the methods discussed in this paper with respect to their ability to *rigorously* treat various properties of Coulomb systems.

| Method    | Strong coupling | Quantum effects | Dynamic properties | Short-times |
|-----------|-----------------|-----------------|--------------------|-------------|
| PIMC      | +++             | ++ <sup>a</sup> | +                  | –           |
| QKinetics | + <sup>b</sup>  | +++             | +++                | +++         |
| MD        | +++             | + <sup>c</sup>  | +++                | +++         |

PIMC: path integral Monte Carlo.

QKinetics: quantum kinetic theory.

MD: classical molecular dynamics.

<sup>a</sup> For fermions only finite temperatures,  $T > 0$ .

<sup>b</sup> Only special classes of strong correlations (e.g. ladder diagrams).

<sup>c</sup> With the use of quantum potentials.

be reduced leading to a reduction of kinetic energy, owing to total energy conservation. A possible realization is demonstrated in figure 5: at  $t \approx 2.5/\omega_{pl}$  the interaction between the particles is reduced so rapidly that they have no time to readjust their arrangement. During a subsequent evolution lasting to about  $t \approx 4/\omega_{pl}$  the plasma responds to this modification: pair correlations are weakened, leading to a reduction of the magnitude of correlation energy and of kinetic energy—the system cools. Such schemes are indeed possible [35], best candidates are two-component plasmas with large mass difference, such as ions in traps or dusty plasmas. For a theoretical description of these processes, again, models are needed which conserve total energy and allow us to describe fast changes in the system: generalized quantum (or classical) kinetic equations and molecular dynamics, more detailed results are given in [35].

#### 4. Conclusion

In this paper, we have discussed correlated quantum Coulomb systems and approaches for a rigorous theoretical and computational treatment. Naturally, only a few concepts have been discussed in some detail which, nevertheless, characterize the present situation in the field:



there exist powerful approaches each of which is capable for a first-principle description of certain limiting cases or certain particular properties of QCS. As sketched in table 1, various schemes have complementary strengths: quantum kinetics is well suited for the treatment of nonequilibrium processes in quantum systems as long as correlations are weak. In contrast, MD has no limitations with respect to the strength of correlations, but is not rigorous (yet) in treating quantum effects. Excellent equilibrium results are delivered by PIMC methods but they cannot easily be extended to nonequilibrium.

Therefore, a very fruitful direction of research appears to find combination of these (and possibly other) theoretical and numerical methods.

## Acknowledgments

MB acknowledges stimulating discussions with J Dufty and W Ebeling. This work has been supported by the Deutsche Forschungsgemeinschaft (BO1366-2) and SFB 198 (B10), by the Deutsche Physikalische Gesellschaft via the Gustav-Hertz-Prize, by a grant for CPU time at the NIC Jülich and a grant from the US Department of Energy.

## References

- [1] Haberland H, Schlages M and Ebeling W (ed) 2001 *Proc. 10th Int. Workshop on the Physics of Nonideal Plasmas Contrib. Plasma Phys.* **41**
- [2] Kalman G (ed) 1998 *Strongly Coupled Coulomb Systems* (Oxford: Pergamon)
- [3] Bonitz M 2002 *Physik Journal* July/August 2002 69–75 (in German)
- [4] Bonitz M 1998 *Quantum Kinetic Theory* (Stuttgart/Leipzig: Teubner-Verlag)
- [5] Kraeft W D, Kremp D, Ebeling W and Röpke G 1986 *Quantum Statistics of Charged Particle Systems* (Berlin: Akademie-Verlag)
- [6] Kadanoff L P and Baym G 1989 *Quantum Statistical Mechanics* 2nd edn (Reading, NA: Addison-Wesley)
- [7] Bonitz M (ed) 2000 *Progress in Nonequilibrium Greens Functions* (Singapore: World Scientific)
- [8] Militzer B and Ceperley D M 2000 *Phys. Rev. Lett.* **85** 1890
- [9] Filinov V S, Bonitz M, Ebeling W and Fortov V E 2001 *Plasma Phys. Contr. Fusion* **43** 743
- [10] Filinov A, Bonitz M and Lozovik Yu 2001 *Phys. Rev. Lett.* **86** 3851
- [11] Filinov V S, Bonitz W M, Levashov P, Fortov V E, Ebeling W, Schlages M and Koch S W 2003 *J. Phys. A: Math. Gen.* **36** 6069–76
- [12] Schlages M, Bonitz M and Tschttschjan A 1995 *Contrib. Plasma Phys.* **35** 109
- [13] Filinov V S, Fortov V E, Bonitz M and Levashov P R 2001 *JETP Lett.* **74** 384 (*Pis'ma v ZhETF* **74** 422)
- [14] Militzer B and Pollock E L 2000 *Phys. Rev. E* **61** 3470
- [15] Filinov V S, Bonitz M and Fortov V E 2000 *JETP Lett.* **72** 245
- [16] Filinov V S, Fortov V E, Bonitz M and Kremp D 2000 *Phys. Lett. A* **274** 228
- [17] Feldmeier H and Schnack J 2000 *Rev. Mod. Phys.* **72** 655
- [18] Knaup M *et al* 2003 *J. Phys. A: Math. Gen.* **36** 6165–71
- [19] Golubnychi V, Bonitz M, Kremp D and Schlages M 2001 *Phys. Rev. E* **64** 016409 (and 2001 *Contrib. Plasma Phys.* **42** 37)
- [20] Hansen J P 1973 *Phys. Rev. A* 3096
- [21] Filinov V S *et al* 2002 *Phys. Rev. B* **65** 165124 and references therein
- [22] Filinov V S, Thomas P, Varga I, Meier T, Bonitz M, Fortov V E and Koch S W 2003 *J. Phys. A: Math. Gen.* **36** 5905–11
- [23] Kwong N H and Bonitz M 2000 *Phys. Rev. Lett.* **84** 1768 and in reference [7], p 418
- [24] Keldysh L V 1965 *JETP* **20** 1018 (1964 *ZhETF* **47** 1515) and in [25]
- [25] Bonitz M and Semkat D (ed) 2003 *Progress in Nonequilibrium Greens Functions II* (Singapore: World Scientific)
- [26] Kremp D, Bornath T, Schlages M and Bonitz M 1999 *Phys. Rev. E* **60** 4725
- [27] Haberland H, Bonitz M and Kremp D 2001 *Phys. Rev. E* **60** 026405
- [28] Bonitz M *et al* 1996 *J. Phys. B: Cond. Matt.* **8** 6057
- [29] Binder R, Köhler S and Bonitz M 1997 *Phys. Rev. B* **55** 5110

- [30] Kwong N H, Bonitz M, Binder R and Köhler S 1998 *Phys. Stat. Sol. (b)* **206** 197
- [31] Filinov A, Bonitz M and Ebeling W 2003 *J. Phys. A: Math. Gen.* **36** 5899–904
- [32] Bonitz M and Kremp D 1996 *Phys. Lett. A* **212** 83
- [33] For an experimental demonstration in semiconductors, see Huber R, Tauser F, Brodschelm A, Bichler M, Abstreiter G and Leitenstorfer A 2001 *Nature* **414** 286
- [34] Semkat D, Kremp D and Bonitz M 2000 *J. Math. Phys.* **41** 7458
- [35] Gericke D O, Murillo M S, Semkat D, Bonitz M and Kremp D 2003 *J. Phys. A: Math. Gen.* **36** 6087–93